Optimal Power Flow in DC Networks with Robust Feasibility and Stability Guarantees

Jianzhe Liu, *Member, IEEE*, Bai Cui, *Member, IEEE*, Daniel K. Molzahn, *Senior Member, IEEE*, Chen Chen, *Senior Member, IEEE*, Xiaonan Lu, *Member, IEEE*, and Feng Qiu, *Senior Member, IEEE*

***Abstract*— With high penetrations of renewable generation and variable loads, there is significant uncertainty associated with power flows in DC networks such that stability and operational constraint satisfaction are of concern. Most existing DC network optimal power flow (DN-OPF) formulations assume exact knowledge of loading conditions and do not provide stability guarantees. In contrast, this paper studies a DN-OPF formulation which considers both stability and operational constraint satisfaction under uncertainty. The need to account for a range of uncertainty realizations in this paper's robust optimization formulation results in a challenging semi-infinite program (SIP). The proposed solution algorithm reformulates this SIP into a computationally tractable problem by constructing a tight convex inner approximation of the feasible region using sufficient conditions for the existence of a feasible and stable power flow solution. Optimal generator setpoints are obtained by optimizing over the proposed convex stability set. The validity and value of the proposed algorithm are demonstrated through various DC networks adapted from IEEE test cases.**

NOMENCLATURE

Parameters

δ	Composite uncertainty
C_ℓ	Capacitance for loads
C_s	Capacitance for sources
L_c	Inductance for power lines
n	Total number of components
n_ℓ	Total number of loads
n_s	Total number of generators
n_c	Total number of power lines
p_ℓ^*	Nominal power injection of loads
p_ℓ	Power injection of loads
R_ℓ	Resistance for loads
R_c	Resistance for power lines
R_s	Resistance for sources
$Y_{\ell\ell}$	Admittance submatrix for load connectivity
$Y_{\ell s}$	Admittance submatrix for load-generator connectivity

sets

Δ	Perturbation set
$\mathcal{E}_\mathrm{c}$	Index set of power lines
$\mathcal{N}_\ell$	Index set of loads
$\mathcal{N}_s$	Index set of generators
$\mathcal{P}_\ell$	Set of load profiles
$\mathcal{V}^\mathrm{ref}$	Generator voltage set-point constraint set
$\mathcal{V}_\ell$	Generator voltage set-point constraint set

Variables

I_c	Power line current at equilibrium
$i_\mathrm{c}(t)$	Current through power lines
$i_d(t)$	Current flowing out of power line
$i_o(t)$	Current flowing into power line
V^ref	Voltage set-point for generators
V_ℓ	Load terminal voltage at equilibrium
V_s	Generator terminal voltage at equilibrium
$v_\ell(t)$	Voltage across capacitor of loads
$v_s(t)$	External voltage of generators
x	System states
x^e	System equilibrium

This work was authored in part by the National Renewable Energy Laboratory, operated by Alliance for Sustainable Energy, LLC, for the U.S. Department of Energy (DOE) under Contract No. DE-AC36-08GO28308. This work was supported by the Laboratory Directed Research and Development Program at the National Renewable Energy Laboratory. The views expressed in the article do not necessarily represent the views of the DOE or the U.S. Government. The U.S. Government retains and the publisher, by accepting the article for publication, acknowledges that the U.S. Government retains a nonexclusive, paid-up, irrevocable, worldwide license to publish or reproduce the published form of this work, or allow others to do so, for U.S. Government purposes.

J. Liu and F. Qiu are with the Energy Systems Division, Argonne National Laboratory, Lemont, IL 60439, USA. Email: {jianzhe.liu, fqiu}@anl.gov. Argonne National Laboratory's work is based upon work supported by the U.S. Department of Energys Office of Energy Efficiency and Renewable Energy (EERE) under the Solar Energy Technologies Office Award Number 34230.

B. Cui is with the Power Systems Engineering Center, National Renewable Energy Laboratory, Golden, CO 80401, USA. Email: bcui@nrel.gov.

D. Molzahn is with the School of Electrical and Computer Engineering, Georgia Institute of Technology, Atlanta, GA 30332, USA. Email: molzahn@gatech.edu.

C. Chen is with the School of Electrical Engineering, Xi'an Jiaotong University, Shaanxi, China. Email: morningchen@xjtu.edu.cn. His work was performed while working with Argonne National Laboratory.

X. Lu is with the College of Engineering, Temple University, Philadelphia, PA 19122, USA. Email: xiaonan.lu@temple.edu.

I. INTRODUCTION

Recent years have witnessed the growth of DC loads and generators, such as DC fast charging facilities, photovoltaic generation, and various electronic devices in sites like data centers. Interconnecting DC components in a DC network is an efficient operation method due to the reduction of DC-AC conversion stages [1]. DC networks have thus found promising applications in low- and medium-voltage power systems such as community nanogrids and microgrids, shipboard power systems, data centers, etc. [2]. Common features of DC networks include: 1) the uncertainty in loading conditions

is usually more significant due to the higher penetration level of uncertain components and relatively smaller scale compared to AC networks, and 2) many loads are controlled as constant power loads (CPLs) that have a destabilizing negative resistance effect that reduces the damping in a system [2].[1]

Similar to other power systems, a DC network should work at a stable operating point that satisfies all operational constraints. The classic method to compute such an operating point is to formulate and solve an optimal power flow (OPF) problem. An OPF problem finds the optimal generation schedule corresponding to the system operating point that maximizes economic welfare while satisfying various physical and operational constraints.

Solving OPF problems to optimality with an AC power flow model is generally challenging due to the associated nonconvexity [4]. Many research efforts have been devoted to improve OPF tractability using approximation and relaxation methods [5]. Recent research has also studied OPF problems for DC networks (DN-OPF) [6]–[11]. Note that DN-OPF problems are fundamentally different from the so-called "DC-OPF" problems [12]: 1) A DC-OPF problem is a simplified OPF problem for an AC system where the nonlinear AC power flow equations are linearized. Conversely, a DN-OPF problem considers the nonlinear power flow equations that accurately model the physics of a DC network. 2) While a DC-OPF problem is usually convex, a general DN-OPF problem is a nonconvex optimization problem [9].

A variety of methods have been applied to solve DN-OPF problems. In [6], a genetic algorithm is applied to solve the OPF problem for a DC distribution system. In [13], linearization techniques are used to simplify the problem. Other methods [7], [8] employ second-order cone programming (SOCP) and quadratic convex programming to relax a DN-OPF problem into a convex formulation. The existing works demonstrate the capability to effectively solve various deterministic DN-OPF problems.

Despite recent advances, existing DN-OPF works in the literature have limitations in providing stability and feasibility guarantees when significant uncertainties are present. First, previous results primarily focus on deterministic DN-OPF problems where the loading conditions are assumed to be fixed and known *a priori*. Nevertheless, with high penetrations of intermittent generation and variable loads, uncertainty in the net loading conditions is a salient feature of DC networks [14]. Directly applying the OPF decisions computed using a specific scenario to an uncertain system can cause unpredictable deviations of the system operating point from the designated value [15], [16]. This may lead to violations of operational constraints and possibly cause voltage collapse. For example, unexpected DC fast charging events or loss of renewable generation can make the system unable to accomplish the load-supporting task, in which case the power flow equations cease to admit a solution [17], [18].

Second, previous results do not consider stability issues of DN-OPF solutions. A DC network has rich dynamics contributed by electrical circuits and control systems [1], which are subject to notable risks of instability associated with the choice of operating points [19]–[22]. Many loads in a DC network can be considered as CPLs that are known to have harmful negative impedance effects. If the operating point is not carefully selected, the system can be under-damped or even become unstable [19]. It is worth mentioning that the joint problem of existence and stability of an equilibrium has been studied in control-theoretic work such as [23], [24]. However, these prior works primarily focus on developing feasibility and stability conditions. The literature still lacks a control synthesis approach that not only ensures existence and stability of the equilibrium but also designs the location of the equilibrium, for example, to guarantee the satisfaction of various engineering constraints and achieve economic goals for a DC network.

We propose a stability-constrained robust DN-OPF algorithm to address these limitations. Following DC network operation practices, we focus on a DC network with nonlinear CPLs and controllable voltage sources. We seek to minimize system operational costs by computing setpoints for the sources which rigorously guarantee the following two properties for any loading condition within a specified uncertainty set: 1) robust feasibility (existence of power flow solutions satisfying operational constraints) and 2) robust stability (local exponential stability of the operating point).

To provide such guarantees, we formulate a DN-OPF problem that incorporates robust feasibility and stability conditions. Solving this problem is difficult. First, existing stability conditions for DC networks are developed to study given operating points [14]; hence, ensuring stability when operating points are decision variables is challenging. Additionally, to ensure robustness, the power flow equations along with the stability conditions need to jointly hold for all uncertainty realizations. This results in a semi-infinite programming (SIP) problem that is generally computationally intractable [25]. Tractable reformulations or approximations exist for robust optimization problems when special structures of problem formulation and data uncertainty can be exploited [26]; however, there are no standard approaches to deal with the nonconvexity associated with the power flow equations.

The proposed algorithm converts the SIP problem into a tractable formulation that resembles a well-studied DN-OPF problem. The main idea of the proposed work is illustrated in Fig. 1, and we summarize the main technical tasks as follows:

(1) We first derive a stability set in the voltage space such that any operating point therein is guaranteed to be stable.
(2) We then develop conditions that guarantee the existence of a power flow solution in a feasibility set for any loading condition. We characterize the boundaries of the feasibility set defined by these conditions.
(3) Finally, we formulate and solve a tractable problem reminiscent of a DN-OPF problem to ensure that the entirety of the set of operating points lies in the intersection of the stability set and the operational constraints.

The contributions of the paper are summarized as follows:

- We develop a novel algorithm to reformulate and solve a class of otherwise intractable DN-OPF problems using a

[1]DC CPLs can be considered as a special case of AC CPLs when the CPLs have a unity power factor. With a non-unity power factor, AC CPLs behave as negative resistances and reactances [3].

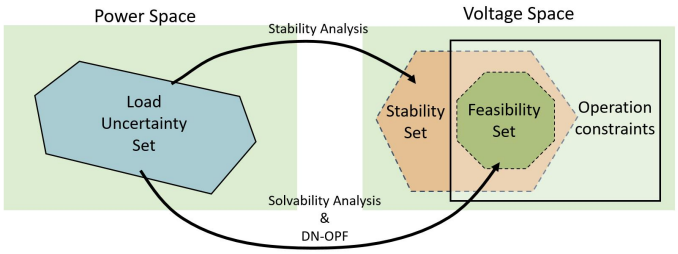

Fig. 1. Illustration of the proposed work.

synthesis of new DC network stability analysis and power flow feasibility results.

- We provide a new condition regarding the solvability of DC network power flow equations and new methods to computing a stability set. The solvability condition establishes an explicit bound on power flow solution (bus voltages) as a function of load powers.
- We provide insights into DC network operations. For example, we provide a rigorous argument for monotonicity in power flow solutions such that the reduction of load power at any bus leads to strictly higher load bus voltages for all load buses.

The rest of the paper is organized as follows: First, Section II introduces the system model and the main problem considered in this paper. Next, Section III shows the main results of the paper, i.e., a solution algorithm for a robust DN-OPF problem with feasibility and stability guarantees. Section IV then demonstrates the efficacy of the proposed work using simulation case studies. Finally, Section V concludes the paper and discusses future research directions.

II. System Modeling and Problem Statement

A. Notation

In this paper, we use $\mathbb{1}$ and $\mathbb{0}$ to represent vectors of all 1's and 0's of appropriate sizes. Recall that a square matrix A is Hurwitz if all real parts of its eigenvalues are negative. For a vector v, let v_k represent its k-th element. Let the operator $\mathrm{diag}\{v\}$ yield a diagonal matrix with the vector's components being the diagonal entries. For a real square matrix A, A^{-1} denotes its inverse, $A \succ 0$ (resp., $A \succeq 0$) means it is symmetric positive definite (resp., semidefinite), and $A \prec 0$ (resp., $A \preceq 0$) means $-A \succ 0$ (resp., $-A \succeq 0$).

B. DC Power Systems

In this paper, we focus on a DC network with n_s generators, n_ℓ loads, and n_c power lines. The total number of these components is $n = n_s + n_c + n_\ell$. Let the index sets of generators, loads, and power lines be $\mathcal{N}_s$, $\mathcal{N}_\ell$, and $\mathcal{E}_c$, respectively. Fig. 2 shows an example DC network consisting of lumped π-equivalent models [22] where generators and loads are interconnected via equivalent RLC circuits [1].

1) Load and Generator Models: Fig. 3 shows a zoomed-in image of one part of the circuit. The lines are represented using a π-equivalent model [22] with a series line resistance and line inductance connected with shunt capacitors at both

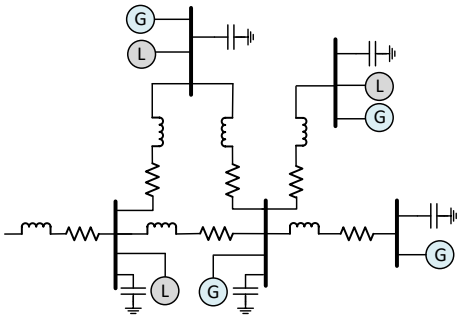

Fig. 2. Example DC power network.

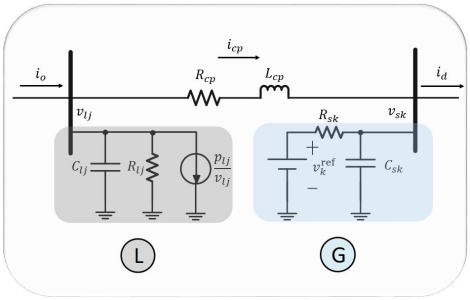

Fig. 3. Zoomed-in image of the dynamic circuit.

ends,[2] and each DC bus has a DC bus capacitor and a shunt resistor. The shunt capacitors are in parallel with the DC bus capacitor. For simplicity, we use one composite shunt capacitor to model their joint effects. Suppose the circuit has the k-th generator, p-th power line, and j-th load. Let $i_o(t)$ and $i_d(t)$ represent the current flowing into and out of the circuit, and let i_{cp} represent the current flow in power line p.

Loads are modeled as constant power injections into the network. We let both constant power loads (CPLs) and constant power sources (CPSs) be connected in parallel. These are non-ideal components with parasitic resistances that are represented as lumped resistors. It is well known that CPLs are nonlinear loads with negative impedance effects. They are the major sources of instabilities in DC networks [2], [20].

For the j-th load, let $p_{\ell j}$ represent its power injection into the network, and let $v_{\ell j}$ represent the terminal voltage. At the nominal condition, $p_{\ell j} = p^*_{\ell j}$, where $p^*_{\ell j}$ is a given constant. Each $p_{\ell j}$ is considered to be a perturbation to $p^*_{\ell j}$ that is unknown and bounded within a given uncertainty interval $[\underline{p}_{\ell j}, \bar{p}_{\ell j}]$. Throughout this paper, we let positive $p_{\ell j}$ represent positive power injection (i.e., power generation) at bus j. We also let $\bar{p}_{\ell j} \geq 0$ to allow loads to be turned off completely. In this paper, the load profile p_ℓ is modeled as an uncertain vector bounded by element-wise interval constraints. Let $\mathcal{P}_\ell$ be the interval uncertainty set, that is, $\mathcal{P}_\ell = \{p_\ell : p_{\ell j} \in [\underline{p}_{\ell j}, \bar{p}_{\ell j}], j \in \mathcal{N}_\ell\}$. This modeling choice is appropriate for typical DC networks in conventional settings. DC networks are often used for medium- and low-voltage power distribution systems [2]. For such systems, the passive load variability is generally

[2]Note that the line resistance, inductance, capacitance are evenly distributed for an ideal power line. The π-equivalent model is a simplified power line model commonly used for DC network stability analysis [1], [27], [28].

spatially uncorrelated. We also note that the time-scale of the RLC dynamics is usually milliseconds to sub-seconds, while that of load variations usually ranges from seconds to minutes. Hence, the load power profile is considered constant in the dynamical model with uncorrelated interval uncertainty.

For the k-th source, let V_k^{ref} be the controllable voltage setpoint, v_{sk} be the external generator voltage, and R_{sk}, C_{sk} represent the source resistance and capacitance, respectively. We impose operational constraints on controllable voltage setpoints such that vector V^{ref}, which includes all voltage setpoints, needs to lie within a given convex constraint set $\mathcal{V}^{\text{ref}}$.

Remark 1 (Generator Model): Generators are modeled as non-ideal voltage sources [22] that are in series with equivalent resistors. The reference voltage set-points are designed by grid operators. We assume that proper low-level controllers [2] have been employed to regulate the terminal voltage of a generator to track a reference setpoint. Consequently, the generator can automatically vary power outputs to respond to changing loading conditions. It is worth mentioning that these generators are different from the CPSs. The power output of a CPS is uncertain, and its terminal voltage does not follow a reference.

Remark 2 (Implication of Uncertainty Model): We elaborate the implication of the uncertainty model on optimization formulation and computation in the following. Modeling the uncertainty as a vector with interval bounds is the only known scenario under which the resulting uncertain SDP constraint, which is used to ensure robust stability, admits a tractable approximation with guaranteed tightness factor [26]. It is worth mentioning that more general uncertainty sets can be directly adopted in the proposed framework as long as a tractable approximation of the uncertain SDP constraint exists, regardless of explicit knowledge of approximation quality. For instance, [29] shows that tractable approximations of uncertain SDP problems can be derived for any polyhedral uncertainty set. It then follows that the proposed approach can be applied to problems with polyhedral uncertainty sets. Since ellipsoids can be well approximated by polytopes, ellipsoidal uncertainty sets, which are commonly employed for the modeling of uncertainty set of renewable power profile, can be handled in the proposed framework as well. However, we use the interval uncertainty model in this paper due to its relevance for DC networks and brevity of exposition.

2) Dynamic Network Model: Sources and loads are connected to DC buses. The buses form a connected graph where a bus is a node and an edge is a π-equivalent power line. We exemplify the modeling approach using the RLC circuit shown in Fig. 3. The state variables of the example circuit are the voltages of the capacitors and the currents through the inductors, namely, $v_{sk}(t)$, $v_{\ell j}(t)$, and $i_{cp}(t)$. The design variables are the output voltages of the sources, $V_k^{\text{ref}}, \forall k \in \mathcal{N}_s$. The dynamics of the circuit are represented by the following model using Kirchhoff's current and voltage laws,

$$\frac{di_{cp}(t)}{dt} = \frac{1}{L_{cp}}\left(v_{\ell j}(t) - R_{cp} i_{cp}(t) - v_{sk}(t)\right), \tag{1a}$$

$$\frac{dv_{sk}(t)}{dt} = \frac{1}{C_{sk}}\left(\frac{V_k^{\text{ref}} - v_{sk}(t)}{R_{sk}} - i_d(t) + i_{cp}(t)\right), \tag{1b}$$

$$\frac{dv_{\ell j}(t)}{dt} = \frac{1}{C_{\ell j}}\left(-\frac{v_{\ell j}(t)}{R_{\ell j}} + i_o(t) - i_{cp}(t) + \frac{p_{\ell j}}{v_{\ell j}(t)}\right). \tag{1c}$$

Equations (1a) and (1b) characterize the behavior of the power line and the source. They are linear in the state and design variables. However, (1c) is nonlinear due to the term, $p_{\ell j}/v_{\ell j}(t)$. Recall that $i_o(t)$ and $i_d(t)$ represent aggregate currents flowing from or into the rest of the network. Each of them is a linear combination of the line currents injections into the load bus or the generator bus.

The modeling approach can be applied to the entire system. By dropping the subscripts indicating variable indices, p_ℓ, v_ℓ, v_s, i_c, V^{ref} represent the vectors of load powers, load voltages, generator external voltages, power line currents, and controllable voltage setpoints, respectively. Let $x = [i_c^\top, v_s^\top, v_l^\top]^\top$ be the vector of state variables and $h(x, p_\ell) = [p_{\ell 1}/v_{\ell 1}, \ldots, p_{\ell n_\ell}/v_{\ell n_\ell}]^\top$.

With the above description and notation, the overall dynamics of the DC grid can be written as follows:

$$\dot{x}(t) = Ax(t) + BV^{\text{ref}} + Ch(x(t), p_\ell), \quad p_\ell \in \mathcal{P}_\ell, \tag{2}$$

where $A \in \mathbb{R}^{n\times n}$, $B \in \mathbb{R}^{n\times n_s}$, and $C \in \mathbb{R}^{n\times n_\ell}$ are constant matrices that are determined by the network topology and RLC circuit parameters through similar methods to those in [14]. This is a well-accepted model for DC network stability studies and has been applied to a variety of applications [2], [30] (e.g., analyses of DC transmission system dynamics [30]).

Remark 3 (Extension): The main results of this paper can be extended to DC networks with other generator and load models. For example, many loads are regulated as constant-current and constant-impedance loads; in addition, recently averaging proportional-integral algorithms [31], [32] have been developed for generator control. They introduce additional linear dynamics, and the developed results can be extended to incorporate them as well.

Let $x^{\text{e}}(p_\ell, V^{\text{ref}}) = [(I_c)^\top, (V_s)^\top, (V_\ell)^\top]^\top \in \mathbb{R}^n$ be an equilibrium of (2). Notice that the equilibrium is a function of the load power profile and source voltage setpoint. For notational simplicity, we drop the arguments in I_c, V_s, and V_ℓ here, and henceforth denote the equilibrium by x^{e}.

When $V_{\ell k} \neq 0, \forall k \in \mathcal{N}_\ell$, the linearized Jacobian matrix of system (2) with respect to x^{e} is given as follows:

$$J(V_\ell, p_\ell) = A - \sum\nolimits_{k\in\mathcal{N}_\ell} \frac{p_{\ell k}}{V_{\ell k}^2} e_k e_k^\top, \tag{3}$$

where $e_k \in \mathbb{R}^n$ is a basis vector with the $(n_c + n_s + k)$-th element being $1/\sqrt{C_{\ell k}}$. The Jacobian matrix is an affine function in each term $p_{\ell k}/V_{\ell k}^2$. The form of this matrix shows that the local stability of an operating point depends on both the CPL power and the steady-state CPL voltage.

From basic control theory [33, Thm. 4.6], an equilibrium x^{e} of (2) is locally exponentially stable if there exists a real $n \times n$ positive definite matrix P that satisfies the following condition:

$$PJ(V_\ell, p_\ell) + J(V_\ell, p_\ell)^\top P \prec 0. \tag{4}$$

If p_ℓ and V_ℓ are given, this condition is a linear matrix inequality (LMI) constraint. However, in our problem, p_ℓ is uncertain, V_ℓ is a variable to be determined, and the coupling between V_ℓ and P is non-polynomial.

3) Power Flow Model: The power flow model describes the steady-state behavior at an operating point of a DC network. The power flow model is obtained by setting the left-hand side of (2) to $\mathbb{0}$ and rearranging terms as

$$p_\ell = \operatorname{diag}\{V_\ell\}\left(Y_{\ell\ell}V_\ell + Y_{\ell s}V^{\mathrm{ref}}\right), \tag{5}$$

where the connectivity between CPL–source and CPL–CPL are described by two admittance matrices $Y_{\ell s} \in \mathbb{R}^{n_\ell \times n_s}$ and $Y_{\ell\ell} \in \mathbb{R}^{n_\ell \times n_\ell}$ [34], which are submatrices of the system admittance matrix Y. Equation (5) is quadratic in state variables V_ℓ and bilinear in design variables V^{ref} and state variables V_ℓ. In general, the power flow model (5) usually introduces computational challenges owing to its nonconvexity [7].

In addition, the system at steady state needs to satisfy operational constraints. In this paper, we require that $V_\ell \in \mathcal{V}_\ell$ and $V^{\mathrm{ref}} \in \mathcal{V}^{\mathrm{ref}}$. Both sets are convex sets that represent system operational requirements such as upper and lower voltage bounds. We limit our presentation to only consider the constraints related to the load voltages and generator setpoints, which are directly relevant to the system stability, in order to simplify the paper's discussion. Other variables like the currents are linear functions of the load voltages and generator voltage setpoints. The proposed algorithm can be easily extended to incorporate constraints on these variables.

C. Problem Statement

From the models discussed above, a poorly designed V^{ref} may 1) result in violations of operational constraints; 2) cause local instability for operating points; and 3) lead to infeasibility of (5) or even loss of equilibrium altogether.

The goal of this work is to choose the value of V^{ref} which minimizes operating costs while guaranteeing that the system is robustly feasible and stable. We make the terms *robustly feasible* and *robustly stable* precise in Definition 1 below:

Definition 1: Given a generator voltage setpoint V^{ref}, system (2) is said to be *robustly feasible* if, for every $p_\ell \in \mathcal{P}_\ell$, the system admits an equilibrium x^{e} which satisfies all operational constraints. The system is said to be *robustly stable* if, for every $p_\ell \in \mathcal{P}_\ell$, there exists a corresponding V_ℓ such that the Jacobian $J(V_\ell, p_\ell)$ is Hurwitz.

Remark 4: Despite the rich literature on robust control [35], [36], a special feature of our problem is that the existence, location, and local stability of the equilibrium state is dependent on the interplay between the parameter uncertainty and the control input, as opposed to a common assumption that the equilibrium is fixed at the origin [23].

Desirable operating points for power systems are usually computed by solving OPF problems [37]. Recently, OPF problems for DC networks (DN-OPF) have been a particular research focus [7], [8], [13]. The formulation of existing DN-OPF problems can be summarized as follows:

$$\textbf{DN-OPF}^*\textbf{:} \quad \min_{V^{\mathrm{ref}} \in \mathcal{V}^{\mathrm{ref}}} f(V^{\mathrm{ref}}, V_\ell^*), \tag{6a}$$

$$\text{s.t.} \quad p_\ell^* = \operatorname{diag}\{V_\ell^*\}\left(Y_{\ell\ell}V_\ell^* + Y_{\ell s}V^{\mathrm{ref}}\right), \tag{6b}$$

$$V_\ell^* \in \mathcal{V}_\ell, \tag{6c}$$

where $p_\ell^* \in \mathbb{R}^{n_\ell}$ is the nominal CPL power profile, V_ℓ^* is the steady-state load voltage at the nominal load condition, and $f : \mathbb{R}^{n_s} \times \mathbb{R}^{n_\ell} \to \mathbb{R}$ is a possibly nonconvex cost function that usually represents the operating cost (e.g., power loss or generation cost).

Since our main results do not depend on the structure of the cost function, we do not explicitly specify the cost functions in this paper in order to simplify our discussion. Our approach can easily accommodate typical OPF cost functions. For example, the case studies in Section IV exemplify generation cost minimizations. The total generation cost is formulated by summing the products of each generator's cost coefficient with its power output. Since the generator power outputs can be found using power flow equations, this choice of objective f can be written in terms of the voltages.

Recently, effective methods have been developed to solve the DN-OPF problem (6) using approximation and convex relaxation techniques [7], [8], [13]. However, problem (6) only considers a fixed loading condition and does not explicitly consider system stability. If the actual load is different from the nominal load, the system's operating point may be unexpected and possibly even unstable.

To address these limitations, we focus on the following problem with explicit constraints guaranteeing robust feasibility and robust stability:

R. DN-OPF SIP:

$$\min_{\substack{V^{\mathrm{ref}} \in \mathcal{V}^{\mathrm{ref}} \\ P \succeq 0}} \quad f(V^{\mathrm{ref}}, V_\ell^*), \tag{7a}$$

$$\text{s.t.} \quad (\forall p_\ell \in \mathcal{P}_\ell)$$

$$PJ(V_\ell(p_\ell), p_\ell) + J(V_\ell(p_\ell), p_\ell)^\top P \prec 0, \tag{7b}$$

$$p_\ell = \operatorname{diag}\{V_\ell(p_\ell)\}\left(Y_{\ell\ell}V_\ell(p_\ell) + Y_{\ell s}V^{\mathrm{ref}}\right), \tag{7c}$$

$$V_\ell(p_\ell) \in \mathcal{V}_\ell, \quad \text{(6b)}, \quad \text{(6c)}. \tag{7d}$$

Compared to problem (6), we add the sufficient stability condition from (4) in order to ensure robust stability. We also require all constraints to hold for all $p_\ell \in \mathcal{P}_\ell$ in order to ensure robust feasibility in the presence of uncertainty. Note that $V_\ell(p_\ell)$ is an implicit variable; with given V^{ref}, $V_\ell(p_\ell)$ is a function of p_ℓ.

Problem (7) is a robust optimization problem involving an LMI constraint with structured uncertainty as in (7b) and nonconvex constraints as in (7c). While tractable reformulations or safe approximations have been identified for some robust conic programming problems with special uncertainty sets [26], there are no known general tractable reformulations or safe approximations for robust nonconvex optimization problems in the form of (7). In fact, it has been shown in [4] that the AC-OPF problem is NP-hard even in the deterministic case. Although DN-OPF is simpler than its AC counterpart, there is no efficient solver with global optimality guarantee as far as we know. Even though standard OPF problems can often be solved with high quality by modern interior point-based solvers despite their theoretical computational complexity, the lack of tractable reformulations and approximations makes solving its robust counterpart difficult. As a result, existing robust OPF formulations almost exclusively adopt power flow models that employ convex relaxation techniques instead of the original nonconvex formulation [15], [38], [39]. To find a

tractable way to search for a feasible solution to (7), we derive an efficient convex inner approximation of the feasible region of problem (7) in the next section.

III. Tractable DN-OPF with Robust Feasibility and Stability Guarantees

In this section, we derive a computationally tractable optimization problem whose feasible region is a convex inner approximation to that of the original problem (7). As illustrated in Fig. 1, the development of the inner approximation consists of three main steps. First, we solve a series of tractable SDPs to find a stability set in $\mathcal{V}_\ell$ such that for any load in $\mathcal{P}_\ell$, the corresponding equilibrium is locally exponentially stable if its load voltages lie in the stability set. Second, based on a power flow solvability technique, we derive a sufficient condition on voltage setpoints V^{ref} such that a feasible power flow solution within operational constraints and stability set exists for every $p_\ell \in \mathcal{P}_\ell$. Third, we formulate a DN-OPF problem which optimizes V^{ref} over $\mathcal{V}^{\text{ref}}$ while satisfying the sufficient condition derived in the second step.

A. Robust Stability Set

The stability set is the feasibility region of the stability condition (4). Due to the infinite number of constraints and the non-polynomial structure, this region is difficult to characterize. Motivated by power system operational constraints, this section describes an interval set which inner approximates this region.

Let $\underline{V}^s_{\ell j}$ and $\bar{V}^s_{\ell j} \in \mathbb{R}^{n_\ell}_+$ represent the lower and upper bounds of an interval set of V_ℓ, denoted as $\mathcal{V}^s_\ell = \left\{V_\ell : \underline{V}^s_{\ell j} \le V_{\ell j} \le \bar{V}^s_{\ell j}, \forall j \in \mathcal{N}_\ell\right\}$. We term $\mathcal{V}^s_\ell$ a "robust stability set" when the following definition applies:

Definition 2: A set $\mathcal{V}^s_\ell$ is called a *robust stability set* if there exists a positive definite matrix P such that the following inequality is satisfied for all $V_\ell \in \mathcal{V}^s_\ell$ and all $p_\ell \in \mathcal{P}_\ell$:

$$PJ\left(V_\ell, p_\ell\right) + J\left(V_\ell, p_\ell\right)^\top P \prec 0. \tag{8}$$

From this definition, if an operating point lies in a robust stability set under load uncertainty set $\mathcal{P}_\ell$, it is locally exponentially stable regardless of specific realization $p_\ell \in \mathcal{P}_\ell$. As shown below, this provides us with the flexibility to remove the coupling between equilibrium and load profiles.

The interval robust stability set facilitates efficient optimization formulation to solve problem (7). In the following subsections, we develop rigorous upper and lower bounds on the load bus voltages under any load uncertainty realization given the generator voltage setpoints V^{ref}. To certify robust stability, one only needs to check that the load bus interval is included in the interval robust stability set, which can be performed in a computationally efficient manner.

1) Superposition: The matrix $J(V_\ell, p_\ell)$ has the following two special features: first, the variable $V_{\ell k}$ and the uncertain parameter $p_{\ell k}$ only exist in pairs on the diagonal entries in the form $-p_{\ell k}/V^2_{\ell k}$; second, each composite term $-p_{\ell k}/V^2_{\ell k}$ only appears once in the matrix. This provides the possibility of applying a superposition method to replace each $-p_{\ell k}/V^2_{\ell k}$ with a new variable.

Let $\delta_k = -p_{\ell k}/V^2_{\ell k}$ and $\delta = [\delta_1, \cdots, \delta_{n_\ell}]^\top$. When $p_{\ell k}$ and $V_{\ell k}$ are subject to box constraints, the vector δ is contained in an interval set as well. Let $\Delta \triangleq \{\delta : \underline{\delta}_k \le \delta_k \le \bar{\delta}_k\}$. We call δ the diagonal perturbation to the system Jacobian and call Δ the diagonal perturbation set. Since $p_{\ell k}$ can be positive or negative, we let $\underline{\delta}_k < 0$ and $\bar{\delta}_k > 0$.

With the above discussed definition, substituting $\delta_k = -p_{\ell k}/V^2_{\ell k}$ into (3) yields a new expression for the system Jacobian, $J(\delta) = A + \sum_{k\in\mathcal{N}_\ell} \delta_k e_k e_k^\top$. Hence, the linearized system matrix is now subject to an affine interval parameter uncertainty. In the following, we denote this matrix as $J(\delta)$. We are interested in finding a diagonal perturbation set whose every element makes the matrix Hurwitz stable, i.e., satisfy the following inequalities:

$$PJ(\delta) + J^\top(\delta)P \preceq 0, \quad \forall \delta \in \Delta. \tag{9}$$

Notice that once this Δ can be found, we can translate it into the desired robust stability set.

For a given Δ, there exist multiple methods to certify whether (9) is satisfied [1], [14]. Most existing methods check multiple "critical scenarios" to certify constraint satisfaction for all scenarios. The existing methods have issues with conservativeness or computational tractability. For example, the condition in [1] tests whether all diagonal elements of the Jacobian matrix are negative, which cannot be satisfied in our case when δ_k is positive. A sufficient condition based on LMI feasibility testing is proposed in [14] that involves 2^{n_ℓ} LMI constraints. While numerical tests reveal that the condition in [14] has advantages with respect to limited conservativeness, practical applicability of this condition is challenging since the number of LMI constraints is exponentially dependent on the dimension of the uncertainty.

Since (9) is a *robust semidefinite programming* problem with interval uncertainty set,[3] Theorem 9.1.2 of [26] can be applied to develop a new condition for DC network stability analysis:

Lemma 1: Given Δ, if there exists $P \succ 0$, $N \prec 0$, and n_ℓ positive scalars $\lambda_1, \cdots, \lambda_{n_\ell}$ that satisfy the following LMI conditions, $J(\delta)$ is always Hurwitz stable for all $\delta \in \Delta$:

$$\begin{bmatrix} N + \sum_{k=1}^{n_\ell} \lambda_k e_k e_k^\top \left(\frac{\bar{\delta}_k - \underline{\delta}_k}{2}\right)^2 & Pe_1 & \cdots & Pe_{n_\ell} \\ e_1^\top P & -\lambda_1 & & \\ \vdots & & \ddots & \\ e_{n_\ell}^\top P & & & -\lambda_{n_\ell} \end{bmatrix} \preceq 0, \tag{10a}$$

$$N \succeq P\left(A + \sum_{k=1}^{n_\ell} e_k e_k^\top \frac{\bar{\delta}_k + \underline{\delta}_k}{2}\right) + \left(A + \sum_{k=1}^{n_\ell} e_k e_k^\top \frac{\bar{\delta}_k + \underline{\delta}_k}{2}\right)^\top P. \tag{10b}$$

The condition in Lemma 1 only involves two LMIs. The decision variables are two $n \times n$ matrices, P and N, as well as n_ℓ scalars λ_j. In total, the condition has $2n^2 + n_\ell$ free scalar variables. Since this number is polynomially dependent on n and n_ℓ, the condition has reasonable scalability.

The reduction in computational complexity may induce concerns regarding conservativeness. One method to evaluate

[3] In a robust semidefinite programming problem, the constraint is bilinear in the uncertainty and the decision variable while it is an LMI in the decision variable if the uncertainties are known constants.

the conservativeness is to compare the volume of the largest sets that the conditions can certify. Compared to Lemma 1 of [14] where the number of LMIs is exponential in the number of loads, numerical tests show that the proposed conditions can certify a set with a volume above 95% of the largest set certifiable by exponentially many constraints. For example, we apply our results to the example DC microgrid detailed in Case Study 2 of [14]. The simulation results are shown in Table I. Notice that in the case study, we consider all pure-load buses and fix the voltage lower bounds, hence the volume of the stability set is indexed by the load power. Higher loads correspond to larger sets and a reduction in the condition's conservativeness. Note that the proposed results can certify a set with a volume over 99.5% relative to the condition with exponentially many LMIs in [14] and shows significant improvements compared to the condition with polynominally many LMIs in Proposition 1 of [14].

TABLE I
VOLUME OF LARGEST CERTIFIABLE ROBUST STABILITY SET

	Lemma 1	Expo. LMIs [14]	Poly. LMIs [14]
Highest Load (kW)	-19.87	-19.96	-18.23

2) Computing the Robust Stability Set: With the proposed stability condition, we are equipped with a tractable method to check whether a given Δ satisfies (9). We would like to find a set Δ with a larger volume to find a larger robust stability set. This essentially involves adjusting the vertices of Δ. We use a line search method to accomplish this goal.

A subsequent question concerns selecting an initial guess for Δ that reduces computational efforts in finding a larger stability set. Rather than arbitrarily choosing an initial guess, we make one suggestion of the initial guess that may find the largest interval stability set in a single shot. This guess covers the entire domain of δ with respect to all possible power flow solutions. The details are provided in Appendix A.

Let the initial guess set be denoted as Δ_0. The volume of Δ can be adjusted by introducing a positive scaling factor α to all the vertices. We denote the set after adjustment as $\Delta = \alpha\Delta_0$. We want to find the largest α that satisfies the condition of Lemma 1. This value is found by solving the following generalized eigenvalue problem (GEVP):

$$\textbf{GEVP:} \quad \max_{\alpha>0, P\succ 0, N\prec 0, \lambda>0} \alpha \quad \text{s. t.} \tag{11a}$$

$$\begin{bmatrix} N+\alpha^2\sum_{k=1}^{n_\ell}\lambda_k e_k e_k^\top \left(\frac{\bar\delta_k-\underline\delta_k}{2}\right)^2 & Pe_1 & \cdots & Pe_{n_\ell} \\ e_1^\top P & -\lambda_1 & & \\ \vdots & & \ddots & \\ e_{n_\ell}^\top P & & & -\lambda_{n_\ell} \end{bmatrix} \preceq 0, \tag{11b}$$

$$N \succeq P(A+\sum_{k=1}^{n_\ell} e_k e_k^\top \frac{\bar\delta_k+\underline\delta_k}{2}) + (A+\sum_{k=1}^{n_\ell} e_k e_k^\top \frac{\bar\delta_k+\underline\delta_k}{2})^\top P. \tag{11c}$$

where $\bar\delta_k$ and $\underline\delta_k$ represent the upper and lower bounds of elements in Δ_0 to simplify our discussion.

A solution that is arbitrarily close to the global optimum can be found for the GEVP problem (11) since it is a quasi-convex problem [40]. For a solution α of (11), we are endowed with a robust stability set as described below.

Proposition 1: Given Δ_0, if α is a solution of (11), $\mathcal{V}_\ell^s$ defined in the following is a robust stability set:

$$\mathcal{V}_\ell^{\rm s} = \{V_\ell : V_{\ell k} \geq V_{\ell k}^{\rm s}, \forall k \in \mathcal{N}_\ell\},$$

where $(V_{\ell k}^{\rm s})^2 = \max\{-\bar p_{\ell k}/(\alpha\underline\delta_k),\ -\underline p_{\ell k}/(\alpha\bar\delta_k)\}$.

Proof: Available in Appendix B ∎

In Proposition 1, we find the lower bound for the steady-state voltage to ensure robust stability. This bound is in line with engineering observations for DC grid stability: with larger load power, the system should be operated at higher voltage levels to reduce the risks of instability.

Remark 5: The value of α is critical for determining the robust stability set. If the initial set discussed in Appendix A is used, the value of α is upper bounded by 1 since the set outer approximates the variation range of the uncertainty. When the solution is obtained as 1, the largest interval stability set can be directly found. Otherwise, a line search algorithm can be developed to approximately solve (11). In the line search process, a finite sequence of semidefinite programming (SDP) problems need to be solved. There exist numerically efficient algorithms to solve SDP problems [40].

B. Solvability Condition

As shown in Fig. 1, after the robust stability set is found, our next task is to ensure: a) the system operates in this set and b) the system complies with all other operational constraints. This task is equivalent to the following robust feasibility problem: we need to compute a voltage setpoint $V^{\rm ref} \in \mathcal{V}^{\rm ref}$ that guarantees the existence of power flow solutions (i.e., solutions to (5)) that are in $\mathcal{V}_\ell^s \cap \mathcal{V}_\ell$ for all $p_\ell \in \mathcal{P}_\ell$.

The problem of certifying the existence and characterizing the range of power flow solutions under uncertain power injections has been studied for the AC power flow model through convex restriction [41]. Due to the intrinsic nonconvexity of AC power flow model, the convexification approach may be conservative. On the other hand, the geometry of DC power flow equations is considerably simpler than its AC counterpart (cf. [42]) so better results may be expected. In fact, we show in this section that for the given interval uncertainty set of power injections, there is an efficient way to *exactly* certify solution existence and characterize their bounds.

We first introduce the following Lemma from [43].

Lemma 2 ([43, Thm. 3]): Given p_ℓ and $V^{\rm ref} > \mathbb{0}$, if (5) is solvable, then there exists a *high-voltage solution* $V_\ell^* > \mathbb{0}$ to (5) such that $V_\ell^* \geq V_\ell$ for all other solutions V_ℓ to (5).

The next Lemma shows the existence and bounds of power flow solutions for any loading condition when the *high-voltage solutions* for the extreme loading conditions are known.

Lemma 3: Let $V_{\ell-}$ be the high-voltage solution for $p_\ell = \underline p_\ell$, then (5) is solvable for all $p_\ell \in \mathcal{P}_\ell$ and the high-voltage solution for any $p_\ell \in \mathcal{P}_\ell$ satisfies $V_\ell(p_\ell) \in [V_{\ell-}, V_{\ell+}]$ where $V_{\ell+}$ is the high-voltage solution for $p_\ell = \bar p_\ell$.

Proof: Available in Appendix C. ∎

Lemma 3 describes a power flow solution existence condition. It states that operating points exist for all $p_\ell \in [\underline{p}_\ell, \bar{p}_\ell]$ if an operating point exists for the high-loading condition. Further, this lemma shows that the high-voltage solutions for any $p_\ell \in \mathcal{P}$ are bounded by those for $\underline{p}_\ell$ and $\bar{p}_\ell$. The next result derives a simple certificate to check if the power flow solution is the high-voltage one under nonnegative power injections.

To facilitate subsequent discussion, we rearrange (5) into the following fixed-point form:

$$V_\ell = G_{p_\ell}(V_\ell) \triangleq E + Z_{\ell\ell}\,\mathrm{diag}\{p_\ell\} r(V_\ell), \tag{12}$$

where we denote $Z_{\ell\ell} = Y_{\ell\ell}^{-1}$, $E = -Y_{\ell\ell}^{-1} Y_{\ell s} V^{\mathrm{ref}}$, and $r(V_\ell) = [1/V_{\ell 1}, \cdots, 1/V_{\ell n_\ell}]^\top$ yields the element-wise reciprocal of vector V_ℓ.

Proposition 2: Let the power injection $p_\ell = \bar{p}_\ell \geq \mathbb{0}$ and source voltage $V^{\mathrm{ref}} > \mathbb{0}$ be given. When

$$||Z_{\ell\ell}\,\mathrm{diag}^{-2}\{E\}\bar{p}_\ell||_\infty < 1,$$

there exists a unique solution to (5) in $[E, +\infty)$.

Proof: Available in Appendix D. ∎

Lemma 3 provides the following two implications that align with engineering observations:

1. (*"Monotonicity" with respect to solution existence*) We only need to verify that the system is solvable at the high-loading condition $\underline{p}_\ell$ to ascertain the existence of power flow solution at any loading condition $p_\ell \geq \underline{p}_\ell$.
2. (*Monotonicity with respect to voltage*) The high- and low-loading solutions jointly define solution bounds for power flow solutions under all loading conditions in between, where the high-loading solution provides the lower bound and low-loading solution provides the upper bound.

These implications help reduce computational efforts in DC network operations. For example, one only needs to examine whether the system has an operating point in the high-loading condition to certify all the other cases. Moreover, these conditions are key for developing a solution algorithm for (7).

C. Robust DN-OPF

As we have characterized a cluster of operating points with respect to given generator setpoints, the remaining task is to design the setpoints to steer the cluster into the desired set (i.e., $\mathcal{V}_\ell^s \cap \mathcal{V}_\ell$) and to reduce system operational costs.

To accomplish these two objectives, an optimization problem can be formulated as

R. DN-OPF*:

$$\min_{V^{\mathrm{ref}} \in \mathcal{V}^{\mathrm{ref}}, s>0} \quad f(V^{\mathrm{ref}}, V_\ell^*), \tag{13a}$$

$$\text{s.t.} \quad \underline{p}_\ell = \mathrm{diag}\{V_{\ell-}\}\left(Y_{\ell\ell} V_{\ell-} + Y_{\ell s} V^{\mathrm{ref}}\right), \tag{13b}$$

$$\bar{p}_\ell = \mathrm{diag}\{V_{\ell+}\}\left(Y_{\ell\ell} V_{\ell+} + Y_{\ell s} V^{\mathrm{ref}}\right), \tag{13c}$$

$$E = -Z_{\ell\ell} Y_{\ell s} V^{\mathrm{ref}},\ E \leq V_{\ell+}, \tag{13d}$$

$$\mathbb{1}\, s \leq E,\ Z_{\ell\ell}\bar{p}_\ell \leq \mathbb{1}\, s^2, \tag{13e}$$

$$V_{\ell-} \in \mathcal{V}_\ell^s \cap \mathcal{V}_\ell,\ V_{\ell+} \in \mathcal{V}_\ell^s \cap \mathcal{V}_\ell, \tag{13f}$$

$$\text{(6b), (6c).} \tag{13g}$$

Constraints (13b) and (13c) represent the DN power flow equations for the high- and low-loading conditions, constraints (13d)–(13e) enforce the condition of Proposition 2, and constraints (13f) and $V^{\mathrm{ref}} \in \mathcal{V}^{\mathrm{ref}}$ ensure the operating points are steered into the desired set.

A solution of (13) yields generator setpoints which ensure robust stability and feasibility, as stated by the following result:

Theorem 1: Any solution of (13) is a feasible point of (7).

Proof: Available in Appendix E. ∎

Theorem 1 shows that the feasibility of (13) implies the feasibility of (7). Problem (13) only contains linear and quadratic constraints whose structure resembles that of a classic DN-OPF problem (6). Thus, existing DN-OPF algorithms can be leveraged to solve (13). We use the following algorithm to summarize the main result of the paper:

Algorithm 1 Find V^{ref} for SIP (7)

Input: System matrices A, B, C, D, load uncertainty set $\mathcal{P}_\ell$, constraint sets $\mathcal{V}_\ell$ and $\mathcal{V}^{\mathrm{ref}}$.

Output: A solution V^{ref}.

Step 1: Construct Δ_0 (e.g., use the suggested set detailed in Appendix A).

Step 2: Solve GEVP (11) to find α and all $V_{\ell k}^{\mathrm{s}}, k \in \mathcal{N}_\ell$.

Step 3: Find robust stability set $\mathcal{V}_\ell^s$.

Step 4: Solve problem (13) to find V^{ref}.

Using Algorithm 1, we can compute generator setpoints that ensure robust stability and feasibility. As previously discussed, the algorithm can be executed efficiently with existing tools.

Remark 6 (Actual Operating Points): Our work can ensure the robust stability and feasibility of the actual operating points. Like a general power system, a DC network usually operates at a high-voltage power flow solution [44]. As discussed in Appendix D, all high-voltage solutions are bounded from above by that of the low-loading condition and from below by that of the high-loading condition. Note that $V_{\ell+}$ is the high-voltage solution at the low-loading condition, hence it is a tight upper bound for the system's high-voltage solutions. In addition, $V_{\ell-}$ is a solution at the high-loading condition, which is element-wise less than or equal to the high-voltage solution. Hence, any high-voltage solution must reside in the range $[V_{\ell-}, V_{\ell+}]$, which is entirely steered into the desired set.

Remark 7 (Conservativeness): Numerical studies show that the proposed approach has limited conservativeness. As shown in Section IV, the interval bound $[V_{\ell-}, V_{\ell+}]$ found through solving (13) usually has no gap with respect to the actual operating point variation range.

Remark 8 (Computational Tractability): Algorithm 1 has limited computational difficulty. Specifically, Step 1 can be approximated by SOCPs as shown in Appendix A. Step 2 involves solving a series of SDPs. There exists computationally efficient algorithms to solve both problems [40]. As discussed in Section III-A, Steps 3 only involves simple algebraic calculations that pose trivial computational burdens. As for Step 4, since problem (13) resembles a standard deterministic DN-OPF problem, we can leverage many existing optimization solvers like IPOPT [45] that have been shown to be effective

for solving OPF problems.

IV. Case Studies

This section demonstrates the validity of the proposed algorithm using simulation case studies. The optimization problems are solved using IPOPT [45], and the simulations are performed in Matlab/Simulink.

A. Efficacy

We first focus on an example DC network whose topology and bus types are the same as the IEEE 14-bus system. The parameters of the DC network given in Table II are chosen according to existing DC network case studies [2], [34]. We let the CPLs vary in [-50kW,0], and impose operational bounds of $[450\ \text{V}, 550\ \text{V}]$ on the generator and CPL voltages, which allows a ± 0.1 p.u. deviation when 500 V is set as base voltage. The objective function minimizes the generation costs at the nominal operating condition, which is set to be -25 kW.

TABLE II
Parameters for the 14-bus DC network case study

R_{sk}	0.05 Ω	R_{lj}	5 Ω	R_{cp}	0.05 Ω
L_{cp}	3mH	C_{sk}	0.75mF	C_{lj}	0.9mF

When we ignore the range of possible uncertainty realizations, the solution to the DN-OPF problem (6) yields setpoints of the five generators as $[481.8, 489.7, 481.2, 480.6, 486.5]$ V. We apply these setpoints and consider a uniform increase in load demands of 2.5 kW every 2.5 seconds. As shown in the middle subfigure of Fig. 4, the system becomes unstable at approximately 38 seconds when the load is 45 kW. This shows the need to consider stability properties for operating point design, especially in systems with significant uncertainties.

In comparison, we formulate the optimization problem (13) using our algorithm. Applying the stability analysis approach developed in Section III-A shows that the system is always robustly stable if the steady-state CPL voltage is higher than 500 V. Problem (13) yields the following setpoints: $[543.5, 550.0, 542.8, 542.1, 549.3]$ V. Using these setpoints results in robust stability for the entire range of load demands, as empirically corroborated by Fig. 4. Observe that the system remains stable when the loads are increased at the same rate as in the previous test. In addition, we test the stability of the system after large load step changes, where all the loads increase from 0 kW to 50 kW in five steps. The simulation results are shown in Fig. 5. The system is still stable despite the large load increases.

B. Conservativeness

Moreover, we show that our approach can recover the exact power flow solution variation range. Aside from the previous scenario with all loads, we further consider the scenarios: all generation case, where power outputs of each constant power component varies in $[0, 50\ \text{kW}]$; all mixed case, where each constant power component varies in $[-50\ \text{kW}, 50\ \text{kW}]$.

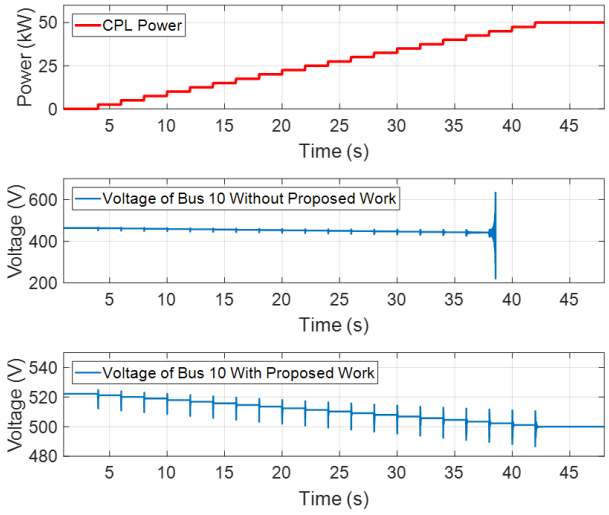

Fig. 4. DC network performance w/ and w/o proposed work

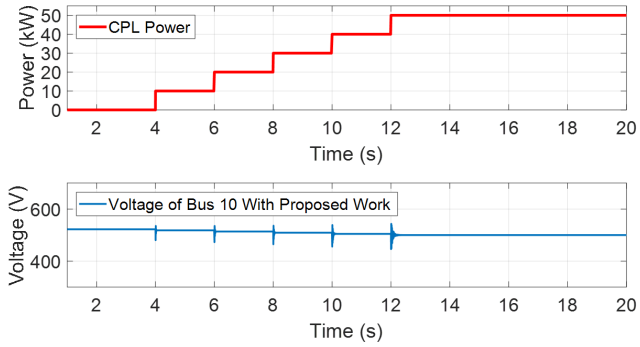

Fig. 5. DC microgrid remains stable with large load variations

Table III presents the difference of the obtained $[V_{\ell-}, V_{\ell+}]$ relative to the actual lower and upper bounds observed in the simulation for the three scenarios. Observe that we find the exact variation range of the system's actual operating points.

TABLE III
Recovering Exact Operating Point Variation Range

	All gen.	All loads	All mixed
Gap for upper bound	0	0	0
Gap for lower bound	0	0	0

C. Computational Efficiency

We have tested the computational tractability of DN-OPF problem (13) on DC networks with the same topology and bus types as the IEEE 9-, 39-, 118-, 300-, and 2383-bus systems. To summarize the results, Table IV compares the average CPU time in IPOPT for solving problem (13) and the traditional DN-OPF problem (6), averaged over 10 tests for each system. Observe that the proposed optimization problem has a similar computational complexity as the traditional DN-OPF problem for systems with moderate sizes, and is

still reasonably tractable for large-scale systems like 2383-bus system. This verifies the tractability of our algorithm.

TABLE IV
COMPARISON OF COMPUTATION TIME (IN SEC.) FOR SOLVING (6) AND (13)

	9-bus	39-bus	118-bus	300-bus	2383-bus
DN-OPF (6)	0.04	0.09	0.17	0.26	0.87
Problem (13)	0.08	0.16	0.50	1.77	196.21

V. CONCLUSION

This paper has developed an algorithm for solving stability-constrained OPF problems in DC networks under uncertainty. Such problems are usually intractable due to infinitely many constraints. Our algorithm uses computationally efficient approaches to transform the problem into a tractable counterpart that resembles a traditional DN-OPF problem such that existing tools can be employed. We first derive a robust stability set within which any operating point is guaranteed to be robustly stable. We then use a sufficient condition which ensures the existence of feasible operating points in this set for all uncertainty realizations in the specified uncertainty set. Low conservativeness and high computational efficiency of the proposed algorithm are demonstrated using various test cases. In future research, we will investigate the application of the algorithm to DN-OPF problems with contingency constraints.

APPENDIX

A. Initial Guess for Robust Stability Set

The suggested set is motivated by the outer convex approximation of an OPF problem. Here we find an outer approximation of the domain of δ. The coupling between p_ℓ and V_ℓ^2 is leveraged to ensure a tight approximation. Let $V_{\ell k+}^2$ and $V_{\ell k-}^2$ be a pair of upper and lower bounds of V_ℓ^2 for any feasible power flow solution, and let δ_{k+} and δ_{k-} be the outer approximation boundaries for δ_k with respect to $V_{\ell k+}^2$ and $V_{\ell k-}^2$. Notice that there are three types of loading conditions: 1) pure-load condition, i.e. $\bar{p}_\ell = 0 \geq \underline{p}_\ell$ (as discussed in Section II-B, $\bar{p}_\ell = 0$ is to allow load to completely turn off); 2) pure-generation condition, i.e. $0 \leq \underline{p}_\ell \leq \bar{p}_\ell$; and 3) mixed condition, i.e. $\underline{p}_\ell \leq 0 \leq \bar{p}_\ell$. We exemplify the choice of the initial guess for the mixed condition here for brevity. Under this condition, $\delta_{\ell j+} = -\underline{p}_{\ell j}/V_{\ell j-}^2$ and $\delta_{\ell j-} = -\bar{p}_{\ell j}/V_{\ell j-}^2$. We only need to find $V_{\ell k-}^2$ in order to obtain δ_{k+} and δ_{k-}. Such a bound can be found through solving the following problem:

$$\textbf{Lower Bound:} \quad \min_{p_\ell \in \mathcal{P}_\ell, V^{\rm ref} \in \mathcal{V}^{\rm ref}} V_{\ell k}^2, \text{ s. t. } (5),\ V_\ell \in \mathcal{V}_\ell. \quad (14)$$

Notice that (14) is a conventional optimal power flow problem with a QCQP formulation. Even though there exist efficient numerical solvers for such problems, the nonconvexity of (14) may still raise concerns regarding the solution of n_ℓ of these problems. Since we only need to find a lower bound on the steady-state voltage, one could instead apply a second-order cone programming (SOCP) relaxation method to find a lower bound of the global optimum of (14).[4]

[4]With certain conditions on the problem structure, the SOCP relaxation of (14) is exact. Detailed discussion can be found in [7], [8].

B. Proof of Proposition 1

Proof: From the definition of Δ, we have $\underline{\delta}_k < 0 < \bar{\delta}_k$ for all $k = 1, \ldots, n_\ell$. Suppose that $\alpha > 0$ and $P \succ 0$ are solutions of GEVP (11). From Lemma 1, any $\delta \in \alpha\Delta_0$ satisfies $PJ(\delta) + J^\top(\delta)P \preceq 0$. Suppose V_ℓ and p_ℓ are arbitrary elements of $\mathcal{V}_\ell^{\rm s}$ and $\mathcal{P}_\ell$, respectively. With a slight abuse of notation, let $\delta = [-p_{\ell 1}/V_{\ell 1}^2, \cdots, -p_{\ell n_\ell}/V_{\ell n_\ell}^2]^\top$. It suffices to demonstrate that $\delta \in \alpha\Delta$ to show the validity of the proposition. For each entry of δ, there are three types of cases to consider: 1) $p_{\ell k} = 0$; 2) $p_{\ell k} > 0$; and 3) $p_{\ell k} < 0$. For case 1), the proof is trivial as $\delta_k = 0$ and it must lie in $[\alpha\underline{\delta}_k, \alpha\bar{\delta}_k]$. For case 2), we have the following derivation, $\alpha\underline{\delta}_k \leq \frac{-\bar{p}_{\ell k}}{(V_{\ell k}^{\rm s})^2} \leq \delta_k = \frac{-p_{\ell k}}{V_{\ell k}^2} < 0 < \alpha\bar{\delta}_k$, where we have used 1) $(V_{\ell k}^{\rm s})^2 \geq -\bar{p}_{\ell k}/(\alpha\underline{\delta}_k)$; 2) $\underline{\delta}_k < 0 < \bar{\delta}_k$; 3) $0 < p_{\ell k} \leq \bar{p}_{\ell k}$; and 4) $0 < (V_{\ell k}^{\rm s})^2 \leq V_{\ell k}^2$. The proof in regards to case 3) is similar and is omitted for brevity. ■

C. Proof of Lemma 3

Proof: To facilitate our discussion, we write $Y_{\ell\ell} = Y_{\ell\ell}^{\rm d} + Y_{\ell\ell}^{\rm off}$ where $Y_{\ell\ell}^{\rm d}$ and $Y_{\ell\ell}^{\rm off}$ are the diagonal and off-diagonal parts of $Y_{\ell\ell}$. The power flow equation (5) can then be rearranged as

$$\operatorname{diag}\{V_\ell\}Y_{\ell\ell}^{\rm d}V_\ell = p_\ell - \operatorname{diag}\{V_\ell\}Y_{\ell\ell}^{\rm off}V_\ell - \operatorname{diag}\{V_\ell\}Y_{\ell s}V^{\rm ref}. \quad (15)$$

Since $Y_{\ell\ell}^{\rm d} \succ 0$, we can left-multiply both sides of (15) by $\left(Y_{\ell\ell}^{\rm d}\right)^{-1}$ to obtain the following reformulation of (5):

$$\operatorname{diag}\{V_\ell\}V_\ell = \left(Y_{\ell\ell}^{\rm d}\right)^{-1}\left(p_\ell - \operatorname{diag}\{V_\ell\}Y_{\ell\ell}^{\rm off}V_\ell - \operatorname{diag}\{V_\ell\}Y_{\ell s}V^{\rm ref}\right). \quad (16)$$

Define $W \triangleq \operatorname{diag}\{V_\ell\}V_\ell$, then (16) represents a fixed-point mapping of W which can be written more compactly as

$$W = F_{p_\ell}(W). \quad (17)$$

We know from [43, Lemma 2] that for any p_ℓ there exists a $W_{\max}$ such that $W_{\max} \geq W$ for any W satisfying $W \leq F_{p_\ell}(W)$. In addition, we have $W_{\max} \geq F_{p_\ell}(W_{\max})$. Since $(Y_{\ell\ell}^{\rm d})^{-1}, -Y_{\ell\ell}^{\rm off}, -Y_{\ell s}$ are all positive matrices, $F_{p_\ell}(\cdot)$ is an increasing function: $X \geq Y$ implies $F_{p_\ell}(X) \geq F_{p_\ell}(Y)$. Similarly, $F_{p_\ell}(W)$ is an increasing function with respect to p_ℓ. Let $V_{\ell-}$ be the high-voltage solution for $p_\ell = \underline{p}_\ell$ and denote $\operatorname{diag}\{V_{\ell-}\}V_{\ell-}$ by W_-. Let $p_\ell \geq \underline{p}_\ell$ be given. By monotonicity of F with respect to p_ℓ we know $F_{p_\ell}(W_-) \geq F_{\underline{p}_\ell}(W_-) = W_-$. By definition of $W_{\max}$, we have $W_{\max} \geq F_{p_\ell}(W_{\max})$. Furthermore, $F_{p_\ell}(W_-) \leq F_{p_\ell}(W) \leq F_{p_\ell}(W_{\max})$ holds for any $W \in [W_-, W_{\max}]$ by monotonicity of $F_{p_\ell}(W)$. It follows from the inequalities above that $W_- \leq F_{p_\ell}(W) \leq W_{\max}$ for any $W \in [W_-, W_{\max}]$. In other words, $[W_-, W_{\max}]$ is an invariant set for (17). It follows from Brouwer's fixed-point theorem that (17) admits a fixed point in $[W_-, W_{\max}]$. By definition of $W_{\max}$, the high-voltage solution lies in the set too. We have thus shown that the high-voltage solution exists for all $p_\ell \in \mathcal{P}$ as long as $V_{\ell-}$ exists and it is increasing with respect to load power p_ℓ. The last statement follows. ■

D. Proof of Proposition 2

Proof: Banach's fixed-point theorem is used to establish the proof. It states that for any contraction mapping G on a complete metric space mapping a set to itself, there is a unique point x_0 in the set such that $G(x_0) = x_0$.

We show that $G_{\bar{p}_\ell}(\cdot)$ is a self map on $[E, +\infty)$. Notice that $E > \mathbb{0}$, and $G_{\bar{p}_\ell}(\cdot) = E + Z_{\ell\ell}\,\mathrm{diag}\{\bar{p}_\ell\} r(V_\ell)$ with positive matrix $Z_{\ell\ell}$ and nonnegative $\bar{p}_\ell$. Hence, the second term on the right-hand side must be nonnegative. Thus, for all $V_\ell \in [E, +\infty)$ we have $G_{\bar{p}_\ell}(V_\ell) \geq E$.

Next, we show that $G_{\bar{p}_\ell}(\cdot)$ is a contraction mapping on $[E, +\infty)$. For any $V^a, V^b \in [E, +\infty)$, the infinity norm of $G_{\bar{p}_\ell}(V^a) - G_{\bar{p}_\ell}(V^b)$ is upper bounded as follows:

$$\begin{aligned} &||G_{\bar{p}_\ell}(V^a) - G_{\bar{p}_\ell}(V^b)||_\infty \\ &= ||Z_{\ell\ell}\,\mathrm{diag}\{\bar{p}_\ell\}\left(r(V^a) - r(V^b)\right)||_\infty \\ &\leq ||Z_{\ell\ell}\,\mathrm{diag}^{-2}\{E\}\bar{p}_\ell||_\infty \cdot ||V^a - V^b||_\infty, \end{aligned} \tag{18}$$

where $||Z_{\ell\ell}\,\mathrm{diag}^{-2}\{E\}\bar{p}_\ell||_\infty$ is a positive constant less than 1. Hence, $G_{\bar{p}_\ell}(\cdot)$ is a contraction mapping on $[E, +\infty)$.

From the Banach fixed-point theorem, $G_{\bar{p}_\ell}(\cdot)$ has a unique fixed point in $[E, +\infty)$, which is clearly the high-voltage solution. ∎

E. Proof of Theorem 1

Proof: Suppose V^{ref}, $V_{\ell-}$, $V_{\ell+}$, and s are solutions of (13). We only need to show V^{ref} ensures robust stability and robust feasibility as defined in Definition 1.

First, when (13) is feasible, the condition of Proposition 2 is satisfied with infinity-norm since constraints (13b)–(13e) hold. Lemma 3 says that there must exist a power flow solution V_ℓ in $[V_{\ell-}, V_{\ell+}]$ for any $p_\ell \in [\underline{p}_\ell, \bar{p}_\ell]$.

Second, from (13f) the interval $[V_{\ell-}, V_{\ell+}]$ belongs to $\mathcal{V}_\ell^s \cap \mathcal{V}_\ell$. Hence, the power flow solution $V_\ell \in \mathcal{V}_\ell^s \cap \mathcal{V}_\ell$ as well. Thus, the system power flow solution satisfies both the operational constraints and the stability constraints.

Since $V_\ell \in \mathcal{V}_\ell$ and $V^{\mathrm{ref}} \in \mathcal{V}^{\mathrm{ref}}$, the system is robustly feasible. Since $V_\ell \in \mathcal{V}_\ell^s$, by Proposition 1 the system is also robustly stable. Thus, the proof is complete. ∎

REFERENCES

[1] F. Dörfler, J. W. Simpson-Porco, and F. Bullo, "Electrical networks and algebraic graph theory: Models, properties, and applications," *Proc. IEEE*, vol. 106, no. 5, pp. 977–1005, May 2018.

[2] T. Dragičević *et al.*, "DC microgrids—Part I: A review of control strategies and stabilization techniques," *IEEE Trans. Power Electro.*, vol. 31, no. 7, pp. 4876–4891, Jul. 2016.

[3] E. Hossain, R. Perez, A. Nasiri, and S. Padmanaban, "A comprehensive review on constant power loads compensation techniques," *IEEE Access*, vol. 6, pp. 33 285–33 305, 2018.

[4] K. Lehmann, A. Grastien, and P. Van Hentenryck, "AC-feasibility on tree networks is NP-hard," *IEEE Trans. Power Syst.*, vol. 31, no. 1, pp. 798–801, Jan. 2016.

[5] D. K. Molzahn and I. A. Hiskens, "A survey of relaxations and approximations of the power flow equations," *Found. Trends Electric Energy Syst.*, vol. 4, no. 1/2, pp. 1–221, Feb. 2019.

[6] M. Farasat *et al.*, "GA-based optimal power flow for microgrids with DC distribution network," in *Proc. IEEE Energy Convers. Congr. Expo.*, Sep. 2015, pp. 3372–3379.

[7] L. Gan and S. H. Low, "Optimal power flow in direct current networks," *IEEE Trans. Power Syst.*, vol. 29, no. 6, pp. 2892–2904, Nov. 2014.

[8] J. Li *et al.*, "Optimal power flow in stand-alone DC microgrids," *IEEE Trans. Power Syst.*, vol. 33, no. 5, pp. 5496–5506, Sep. 2018.

[9] A. Garcés, "On the convergence of Newton's method in power flow studies for DC microgrids," *IEEE Trans. Power Syst.*, vol. 33, no. 5, pp. 5770–5777, Sept. 2018.

[10] W. Inam *et al.*, "Stability, control, and power flow in ad hoc DC microgrids," in *Proc. IEEE Workshop Control Model. Power Electron.*, Jun. 2016, pp. 1–8.

[11] J. Ma *et al.*, "Transmission loss optimization-based optimal power flow strategy by hierarchical control for DC microgrids," *IEEE Trans. Power Electron.*, vol. 32, no. 3, pp. 1952–1963, Mar. 2017.

[12] B. Stott, J. Jardim, and O. Alsaç, "DC power flow revisited," *IEEE Trans. Power Syst.*, vol. 24, no. 3, pp. 1290–1300, Aug. 2009.

[13] O. D. Montoya *et al.*, "Linear power flow formulation for low-voltage DC power grids," *Elect. Power Syst. Res.*, vol. 163, pp. 375–381, Oct. 2018.

[14] J. Liu, W. Zhang, and G. Rizzoni, "Robust stability analysis of DC microgrids with constant power loads," *IEEE Trans. Power Syst.*, vol. 33, no. 1, pp. 851–860, Jan. 2018.

[15] R. Louca and E. Bitar, "Robust AC optimal power flow," *IEEE Trans. Power Syst.*, vol. 34, no. 3, pp. 1669–1681, May 2019.

[16] D. K. Molzahn and L. A. Roald, "Towards an AC optimal power flow algorithm with robust feasibility guarantees," in *Proc. Power Syst. Comput. Conf.*, Dublin, Ireland, Jun. 2018, pp. 1–7.

[17] J. W. Simpson-Porco, F. Dörfler, and F. Bullo, "Voltage collapse in complex power grids," *Nature Commun.*, vol. 7, 2016, Art. no. 10790.

[18] B. Cui and X. A. Sun, "A new voltage stability-constrained optimal power-flow model: Sufficient condition, SOCP representation, and relaxation," *IEEE Trans. Power Syst.*, vol. 33, no. 5, pp. 5092–5102, Sept. 2018.

[19] N. Barabanov, R. Ortega, R. Gri, and B. Polyak, "On existence and stability of equilibria of linear time-invariant systems with constant power loads," *IEEE Trans. Circuits Syst. I, Fundam. Theory Appl.*, vol. 63, no. 1, pp. 114–121, Jan. 2016.

[20] L. Herrera, W. Zhang, and J. Wang, "Stability analysis and controller design of DC microgrids with constant power loads," *IEEE Trans. Smart Grid*, vol. 8, no. 2, pp. 881–888, Mar. 2017.

[21] D. Zonetti, R. Ortega, and J. Schiffer, "A tool for stability and power-sharing analysis of a generalized class of droop controllers for high-voltage direct-current transmission systems," *IEEE Trans. Control Netw. Syst.*, vol. 5, no. 3, pp. 1110–1119, Sep. 2018.

[22] J. A. Belk, W. Inam, D. J. Perreault, and K. Turitsyn, "Stability and control of ad hoc DC microgrids," in *Proc. 55th IEEE Conf. Decis. Control*, Dec. 2016, pp. 3271–3278.

[23] M. Ikeda, Y. Ohta, and D. D. Šiljak, "Parametric stability," in *New Trends in Systems Theory*, C. Conte, A. M. Perdon, and B. Wyman, Eds. Boston, MA: Birkhauser, 1991, pp. 1–20.

[24] T. Wada, M. Ikeda, Y. Ohta, and D. Šiljak, "Parametric absolute stability of lur'e systems," *IEEE Trans. Automat. Contr*, vol. 43, no. 11, pp. 1649–1653, Nov. 1998.

[25] J. M. Mulvey, R. J. Vanderbei, and S. A. Zenios, "Robust optimization of large-scale systems," *Oper. Res.*, vol. 43, no. 2, pp. 264–281, Mar. 1995.

[26] A. Ben-Tal, L. El Ghaoui, and A. Nemirovski, *Robust Optimization*. Princeton University Press, 2009.

[27] P. Karlsson and J. Svensson, "Dc bus voltage control for a distributed power system," *IEEE Trans. Power Electron.*, vol. 18, no. 6, pp. 1405–1412, 2003.

[28] J. Beerten, S. Cole, and R. Belmans, "Modeling of multi-terminal vsc hvdc systems with distributed dc voltage control," *IEEE Trans. Power Syst.*, vol. 29, no. 1, pp. 34–42, 2013.

[29] J. Zhen *et al.* (2017) Robust optimization for models with uncertain SOC and SDP constraints. [Online]. Available: http://www.optimization-online.org/DB_FILE/2017/12/6371.pdf

[30] G. O. Kalcon *et al.*, "Small-signal stability analysis of multi-terminal VSC-based DC transmission systems," *IEEE Trans. Power Syst.*, vol. 27, no. 4, pp. 1818–1830, Nov. 2012.

[31] D. K. Molzahn *et al.*, "A survey of distributed optimization and control algorithms for electric power systems," *IEEE Trans. Smart Grid*, vol. 8, no. 6, pp. 2941–2962, Nov. 2017.

[32] T. Morstyn, B. Hredzak, G. D. Demetriades, and V. G. Agelidis, "Unified distributed control for DC microgrid operating modes," *IEEE Trans. Power Syst.*, vol. 31, no. 1, pp. 802–812, Jan. 2016.

[33] H. K. Khalil, *Nonlinear Systems*, 3rd ed. Upper Saddle River, NJ: Prentice Hall, 2002.

[34] Z. Liu *et al.*, "Existence and stability of equilibrium of DC microgrid with constant power loads," *IEEE Trans. Power Syst.*, vol. 33, no. 6, pp. 6999–7010, Nov. 2018.
[35] G. Leitmann, "Guaranteed asymptotic stability for some linear systems with bounded uncertainties," *J. Dyn. Syst. Meas. Control*, vol. 101, no. 3, pp. 212–216, 1979.
[36] J. Doyle *et al.*, "State-space solutions to standard H_2 and H_∞ control problems," *IEEE Trans. Autom. Control*, vol. 34, no. 8, pp. 831–847, Aug. 1989.
[37] M. B. Cain, R. P. O'Neill, and A. Castillo, "History of optimal power flow and formulations (OPF paper 1)," Federal Energy Regulatory Commission, Tech. Rep., 2012.
[38] A. Lorca and X. A. Sun, "The adaptive robust multi-period alternating current optimal power flow problem," *IEEE Trans. Power Syst.*, vol. 33, no. 2, pp. 1993–2003, Mar. 2018.
[39] H. Yang *et al.*, "Robust optimization for electricity generation," *INFORMS J. Comput.*, vol. 33, no. 1, pp. 1–16, 2021.
[40] S. Boyd and L. Vandenberghe, *Convex Optimization*. Cambridge University Press, 2004.
[41] D. Lee *et al.*, "Convex restriction of power flow feasibility sets," *IEEE Trans. Control Netw. Syst.*, vol. 6, no. 3, pp. 1235–1245, Sep. 2019.
[42] M. Jeeninga, C. De Persis, and A. van der Schaft. (2020) DC power grids with constant-power loads—Part I: A full characterization of power flow feasibility, long-term voltage stability and their correspondence. [Online]. Available: https://arxiv.org/abs/2010.01076
[43] K. Dvijotham, E. Mallada, and J. W. Simpson-Porco, "High-voltage solution in radial power networks: Existence, properties, and equivalent algorithms," *IEEE Control Syst. Lett.*, vol. 1, no. 2, pp. 322–327, Oct. 2017.
[44] J. W. Simpson-Porco, F. Dörfler, and F. Bullo, "On resistive networks of constant-power devices," *IEEE Trans. Circuits Syst. II, Express Briefs*, vol. 62, no. 8, pp. 811–815, Aug. 2015.
[45] A. Wächter and L. T. Biegler, "On the implementation of an interior-point filter line-search algorithm for large-scale nonlinear programming," *Math. Program.*, vol. 106, no. 1, pp. 25–57, Mar. 2006.

Jianzhe Liu (S'13-M'18) received the B.E. degree in electrical engineering from Huazhong University of Science and Technology, China, in 2012, and the Ph.D. degree in electrical and computer engineering from The Ohio State University, U.S.A., in 2017. Dr. Liu was a visiting scholar at the Department of Energy Technology, Aalborg University, Denmark, in 2017. He has been with Argonne National Laboratory since 2018, first as a postdoctoral researcher and currently as an Energy System Scientist. In 2019, he received the Argonne Outstanding Postdoc Award. His research interests include control and optimization for electric power systems, power hardware-in-the-loop testing, and resilience and reliability study for power electronics enabled systems.

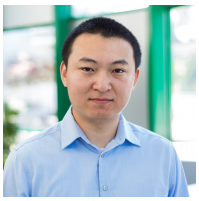

Bai Cui (S'15-M'18) received the B.S. degree in electrical engineering from Shanghai Jiao Tong University, Shanghai, China, in 2011, the B.S. degree in computer engineering from the University of Michigan, Ann Arbor, MI, USA, in 2011, and the Ph.D. degree in electrical and computer engineering from Georgia Institute of Technology, Atlanta, GA, USA, in 2018. He is currently a researcher with the Power Systems Engineering Center at the National Renewable Energy Laboratory (NREL). Prior to joining NREL, he was a postdoctoral appointee at Argonne National Laboratory from 2018 to 2019. His research interests are in optimization and stability analysis of power systems with applications in power system resilience and renewable integration.

Daniel K. Molzahn (S'09-M'13-SM'19) is an Assistant Professor in the School of Electrical and Computer Engineering at the Georgia Institute of Technology and also holds an appointment as a computational engineer in the Energy Systems Division at Argonne National Laboratory. He was a Dow Postdoctoral Fellow in Sustainability at the University of Michigan, Ann Arbor. He received the B.S., M.S., and Ph.D. degrees in electrical engineering and the Masters of Public Affairs degree from the University of Wisconsin–Madison, where he was a National Science Foundation Graduate Research Fellow. He received the IEEE Power and Energy Societys 2021 Outstanding Young Engineer Award for contributions to the theory and practical application of nonlinear optimization algorithms for electric power systems.

Chen Chen received the B.S. and M.S. degrees from Xian Jiaotong University (XJTU), Xian, China, in 2006 and 2009, respectively, and the Ph.D. degree in electrical engineering from Lehigh University, Bethlehem, PA, USA, in 2013.

He is currently a Professor with the School of Electrical Engineering, XJTU. Prior to joining XJTU, he has over six-year service at Argonne National Laboratory, Lemont, IL, USA, with the last appointment as an Energy Systems Scientist with Energy Systems Division. His research interest includes power system resilience, distribution systems and microgrids, demand side management, and communications and signal processing for smart grid. He is also the recipient of the IEEE PES Chicago Chapter Outstanding Engineer Award in 2017. He is an Editor of IEEE TRANSACTIONS ON SMART GRID and IEEE POWER ENGINEERING LETTERS.

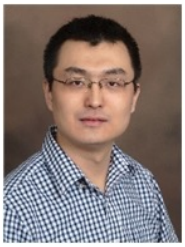

Xiaonan Lu (S'12-M'13) received his B.E. and Ph.D. degrees in electrical engineering from Tsinghua University, Beijing, China, in 2008 and 2013, respectively. From September 2010 to August 2011, he was a guest Ph.D. student at the Department of Energy Technology, Aalborg University, Denmark. From October 2013 to December 2014, he was a Postdoc Research Associate at the Department of Electrical Engineering and Computer Science, University of Tennessee, Knoxville. From January 2015 to July 2018, he was with Argonne National Laboratory, first as a Postdoc Appointee and then as an Energy Systems Scientist. In July 2018, he joined the College of Engineering at Temple University as an Assistant Professor. His research interests include modeling and control of power electronic inverters, hybrid AC and DC microgrids, and real-time hardware-in-the-loop simulation.

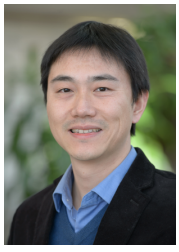

Feng Qiu received his Ph.D. from the School of Industrial and Systems Engineering at the Georgia Institute of Technology in 2013. He is a principal computational scientist and a section leader with the Energy Systems Division at Argonne National Laboratory. His current research interests include power system modeling and optimization, electricity markets, power grid resilience, machine learning and data analytics.